Project acronym:	Geo-Drill		
Project title:	Development of novel and Cost-Effective drilling technology for geothermal Systems		
Activity:	LCE-07-17-Renewables		
Call:	H2020-LC-SC3-2018-RES-TwoStages		
Funding Scheme:	RIA	**Grant Agreement No:**	815319
WP7	Simulation, KBS and DSS		

D7.3 Drill Monitoring Calculator

Due date:	31/08/2022 (M41)	
Actual Submission Date:	5/10/2022	
Lead Beneficiary:	FPS	
Main authors/contributors:	FPS	
Dissemination Level[1]:	PU	
Nature:	Report	
Status of this version:		**Draft under Development**
		For Review by Coordinator
	X	**Submitted**
Version:	01	
Abstract	The report describes the development of a calculator that would support the drill monitor	

REVISION HISTORY

Version	Date	Main Authors/Contributors	Description of changes
v01	30.09.2022	FPS	First version

Funded by the Horizon 2020 Framework Programme of the European Union

1

Dissemination level security:

PU – Public (e.g. on website, for publication etc.) / **PP** – Restricted to other programme participants (incl. Commission services) /

RE – Restricted to a group specified by the consortium (incl. Commission services) / **CO** – confidential, only for members of the consortium (incl. Commission services)

GEODRILL

This project has received funding from the European Union's Horizon 2020 program Grant Agreement No 815319. This publication reflects the views only of the author(s), and the Commission cannot be held responsible for any use which may be made of the information contained therein.

Document: D7..3 Report on Drill Monitor Calculator

Version: 1

Date: 5/10/2022

Summary

A new powerful engineering analysis software for geothermal flow assurance is under development by Flowphys AS. This software is capable of simulating single-phase and multi-phase dynamic (time-dependent) flows in complex pipe networks and is based on conservation equations. Part of the software development is carried out in several H2020 projects: GeoCoat, GeoSmart, GeoPro, GeoDrill, and Eurostars ProCase.

In previous reports D7.1 [1] and D7.2 [2], the 1D multiphase flow assurance and the 1D structural dynamics simulators were described. In the current report, 3D time-dependent turbulent flow simulations have been performed to investigate annulus flows that also includes a rotating drill string. Moreover, the presented method is general and can be used to calculate pressure drops past tool joints, sensor assemblies, etc.

This report should be seen as "part 1" and will be amended with additional models and simulations once experimental data from the Geo-Drill testing campaign becomes available.

Document: D7..3 Report on Drill Monitor Calculator

Version: 1

Date: 5/10/2022

CONTENTS

1. INTRODUCTION

To simulate drilling operations requires multi-physics simulations, as it includes fluid flow, heat transfer, and structural dynamics. Geo-Drill report D7.1, "Geothermal Well Flow Assurance Simulator" [1], describes the fundamentals of a new 1D FEM Geothermal Flow Assurance simulator software that includes annulus flow, non-Newtonian fluids, and a model for the DTH tool. Many other features are included in the software, for example coupling to the computational geochemistry software PHREEQC [3], simulation of reaction kinetics, devices such as pumps, valves, thermodynamics, heat transfer, and more. However, the models implemented are incomplete in that they do not include drill string rotation nor any method for dealing with geometrical differences on the drill string or in the wellbore. To remedy this, a method for flows in general (also complicated) 3D geometries is shown, with application to a rotating drill string. Especially, with this approach it is possible to create fast models (0D/1D or meta-models) suitable for implementation into the 1D software.

2. 3D SIMULATION METHOD

In this report the fluids are assumed to be viscous and incompressible. All CFD computations were carried out with the FlowPhys software, which uses a finite element semi-implicit fractional step approach to solve for the incompressible Navier-Stokes equations. The time-stepping algorithm consists of a 4-steps explicit Runge-Kutta algorithm for the convection terms combined with an implicit Crank-Nicholson algorithm for the diffusion terms, while the pressure is solved implicitly through a pressure Poisson equation. For more details of the algorithm, see GeoDrill D4.1 [4] and Kjellgren [5].

<u>Turbulence modelling through LES approach</u>

Large Eddy Simulation (LES) is used for the turbulence modelling. While the software has several different LES turbulence models implemented, only the constant Smagorinsky coefficient model has been used in this report, as it is the fastest and easiest one to use.

3. 1D & 3D ANNULUS FLOWS

3.1 3D simulations of flows in an annulus

A finite element model of a section of the annulus was created, as is shown in Figure 3.1. The length of the section was 0.5 m, the inner diameter 100 mm and the outer diameter 150 mm. The turbulent flow field develops along the length of the drill pipe, but rather than modelling a very long section of the annulus which would be computationally expensive, periodic boundary conditions have been used, such that the computational model can be kept small (few nodes & elements) and instead the flow field develops with time.

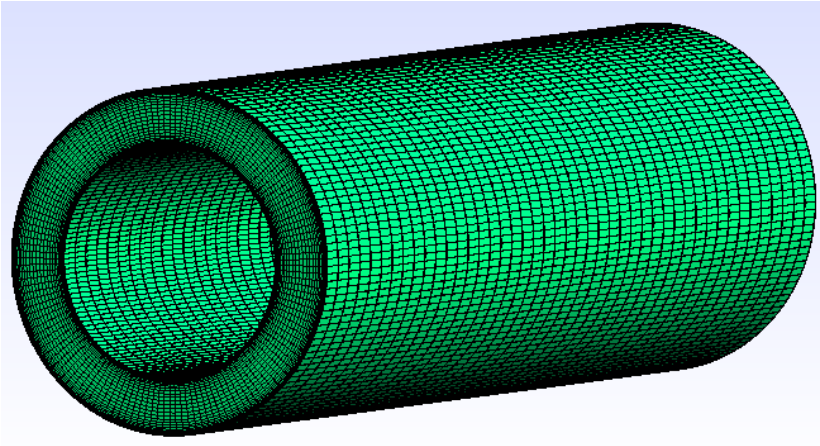

Figure 3.1: Computational mesh of annulus

Computations have been carried out on three different meshes to check grid-convergence. Moreover, 5 different levels of pressure drop, as summarized in Table 1, have been used.

Table 3.1: 3D simulation cases

Pressure Drop [Pa/m]	Flow Regime
0.0097	Laminar
0.0778	Laminar
3.888	Turbulent
15.52	Turbulent
62.208	Turbulent

For laminar flow cases, the transient computations rather quickly stabilize to a steady-state flow field, see Figure 3.2. For the turbulent flow cases, which all were analyzed using Large Eddy Simulation (LES), the flow field remains unsteady with fluctuations. Therefore, to make certain that the flow field is fully developed, time-histories of the bulk velocity is tracked and flow data is only sampled after the bulk velocity has stabilized, i.e. after time t > 150 s in Figure 3.3.

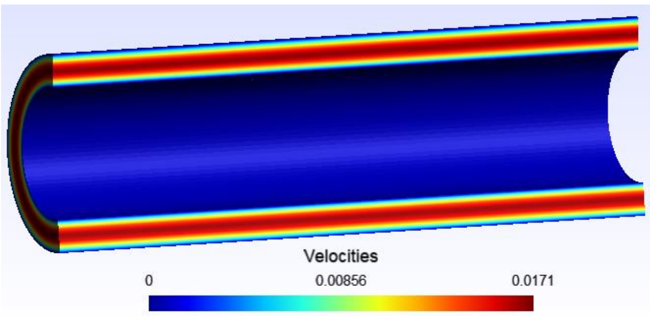

Figure 3.2: Velocity contours for laminar case (domain cut in half for visualization)

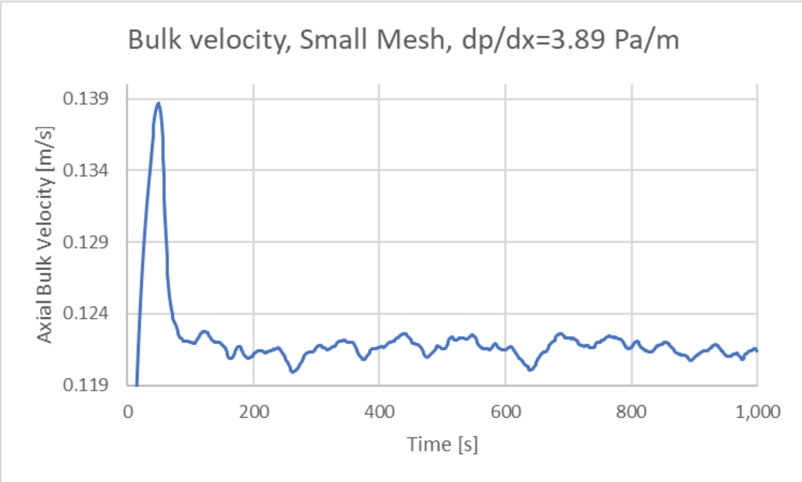

Figure 3.3: Time history of bulk velocity. Flow data is sampled after the flow field has stabilized (t > 150 s for this case)

Sample results for the case with a constant average pressure gradient of dp/dx=3.89 Pa/m are shown in Figure 3.4. Notice that the hydrostatic as well as the average axial pressure gradients have been filtered out for easier visualization of the pressure fluctuations. Moreover, the right-hand figure shows only half of the domain, also for easier visualization.

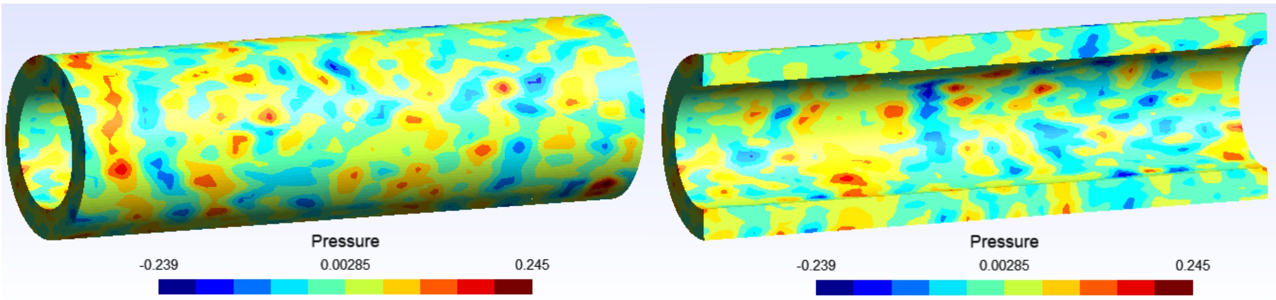

Figure 3.4: Pressure contours for dp/dx= 3.89 Pa/m

Constant velocity contours as well as velocity iso-surfaces are shown in Figure 3.5. Notice that the iso-surfaces show turbulent structures that are stream wise.

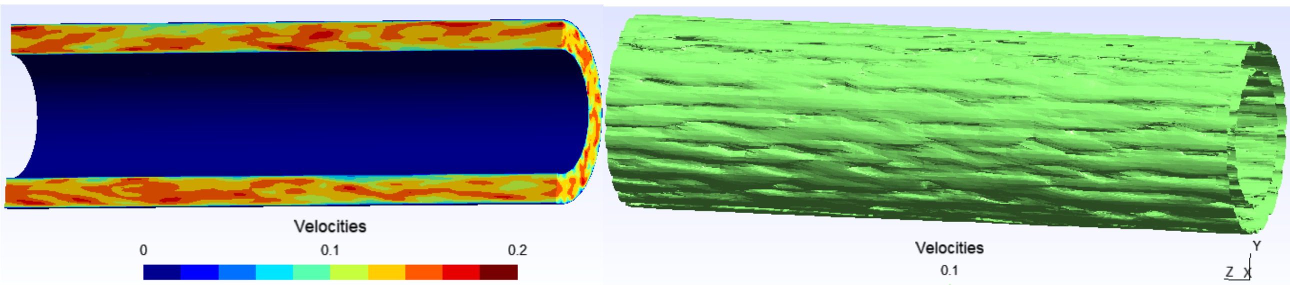

Figure 3.5: Velocity contours and velocity iso-surfaces for the case with dp/dx=3.89 Pa/m

Similarly, results for dp/dx=15.6 Pa/m and dp/dx=62.2 Pa/m are shown in Figures 3.6-3.7. Notice that the higher pressure drops leads to higher bulk velocities as well as larger velocity and pressure fluctuations.

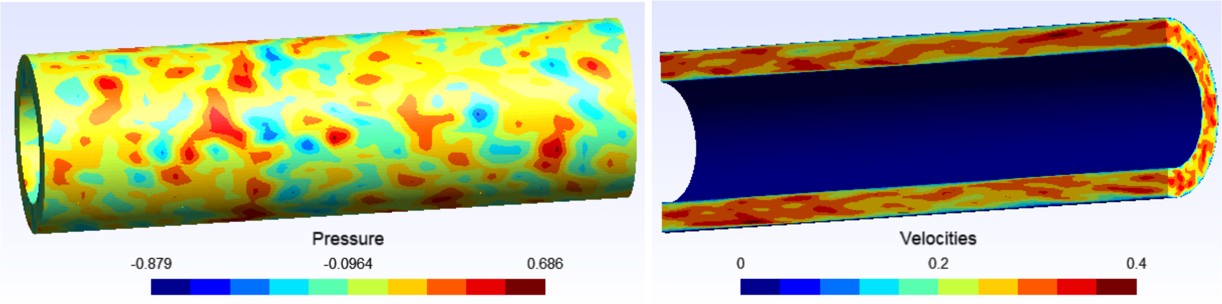

Figure 3.6: Pressure contours for dp/dx= 15.6 Pa/m

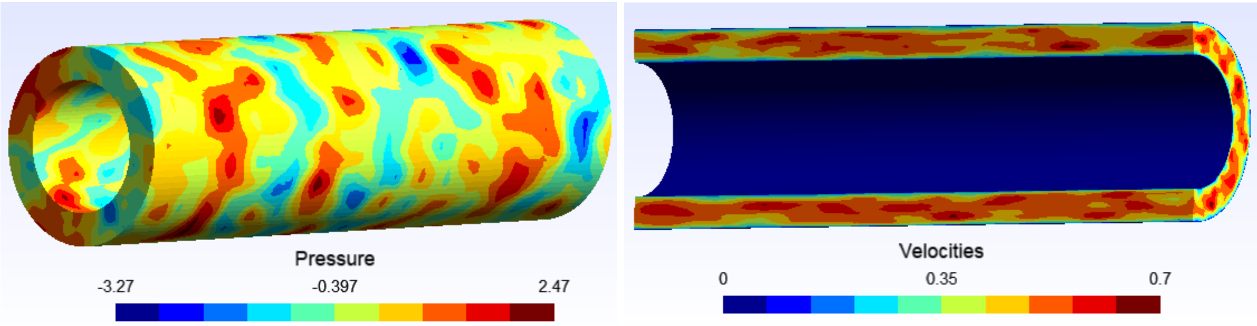

Figure 3.7: Pressure contours for dp/dx= 62.2 Pa/m

3.2 Comparison of 1D and 3D simulations of flows in an annulus

A model for the pressure loss of flow in a concentric annulus was presented in D7.1. In this model, the pressure loss in a circular pipe is calculated as

$$\Delta p = f\rho \frac{Lv^2}{2D} \tag{3.1}$$

where f is the Darcy-Weisbach friction factor, and the pressure loss in a concentric annulus is calculated is calculated in the same way, but with a correction to the friction factor:

$$f_{annulus} = k_g f \tag{3.2}$$

where k_g is a geometric correction factor that is dependent on the diameter ratio Dr=Di/Do, where Di is the annulus' inner diameter, and Do is the outer diameter. This model is used to calculate the pressure losses in the 1D pipe network simulator software.

For the 3D calculations, because periodic boundary conditions are used, it is necessary to set a pressure drop to drive the flow. This pressure drop is set as a source term and added to the Navier-Stokes equations. The viscous shear stresses on the inner and outer surfaces of the annulus will then balance the forces of the pressure drop. Comparison of the resulting bulk flow velocities for given pressure drops using the 1D and the 3D simulations are shown in Figure 3.8. Different mesh densities have been used, and as can be expected, the results agree very well for low Reynolds number, while for higher Reynolds number 3D LES turbulent simulations the mesh density will have a larger influence on the accuracy.

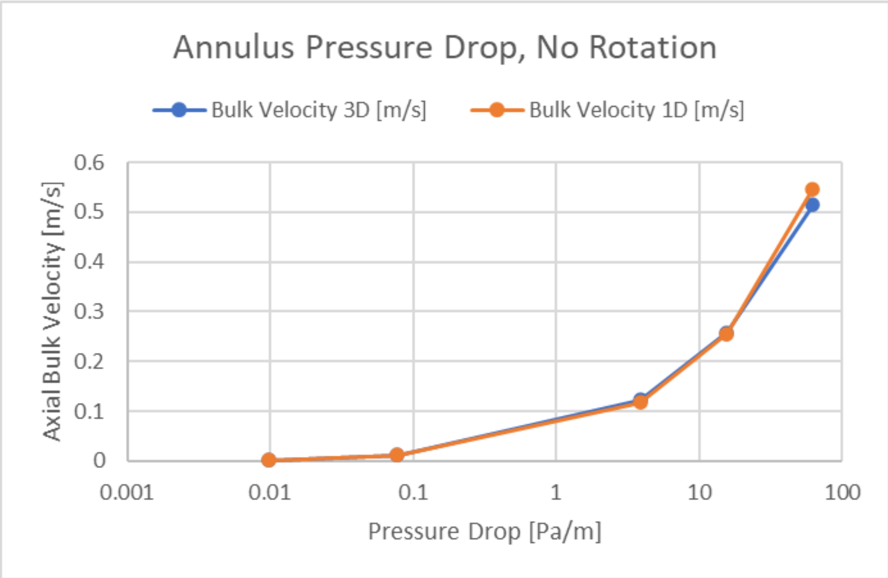

Figure 3.8: Comparison of results for 1D and 3D simulations

4. 1D & 3D ANNULUS FLOWS WITH ROTATING DRILL STRING

4.1 3D simulations of flows in an annulus with rotating drill string

The calculations for the annulus flows in the previous section have been repeated but with a rotating drill string, which is simulated by moving wall boundary conditions on the annulus' inner surface. Ten cases with different pressure drops and rotational speeds have been analyzed, with rotational speeds varying from 5.57 rpm to 44.56 rpm, and pressure drops dp/dx=3.9-62.2 Pa/m.

Results for the largest rotation speed and largest pressure drop (i.e. flow velocity) are shown in Figure 4.1. Notice that the rotating drill string cause the flow field to swirl, with higher velocities on the outside (wellbore) wall than on the inner (drill string) wall. Notice also how the flow structures shown in the velocity iso-surface plot in Figure 4.2 are clearly shaped by the swirl.

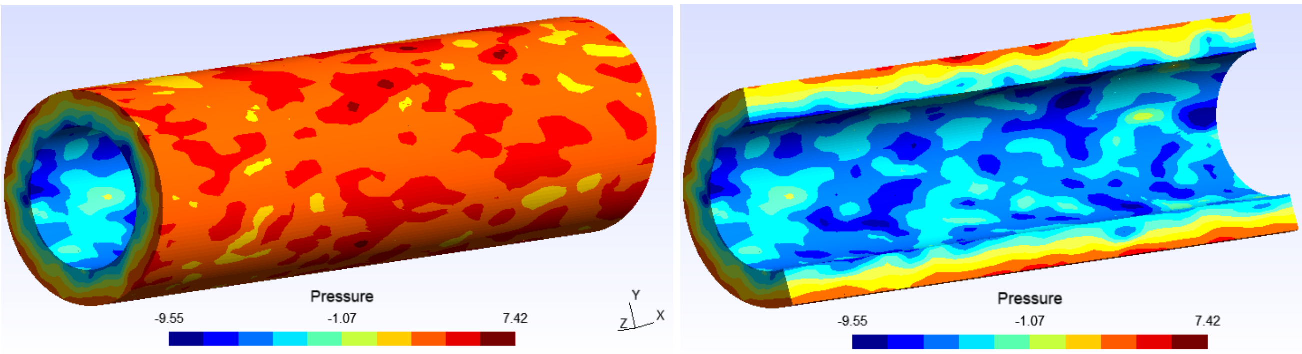

Figure 4.1: Pressure contours for dp/dx= 62.2 Pa/m and rotation 44.6 rpm

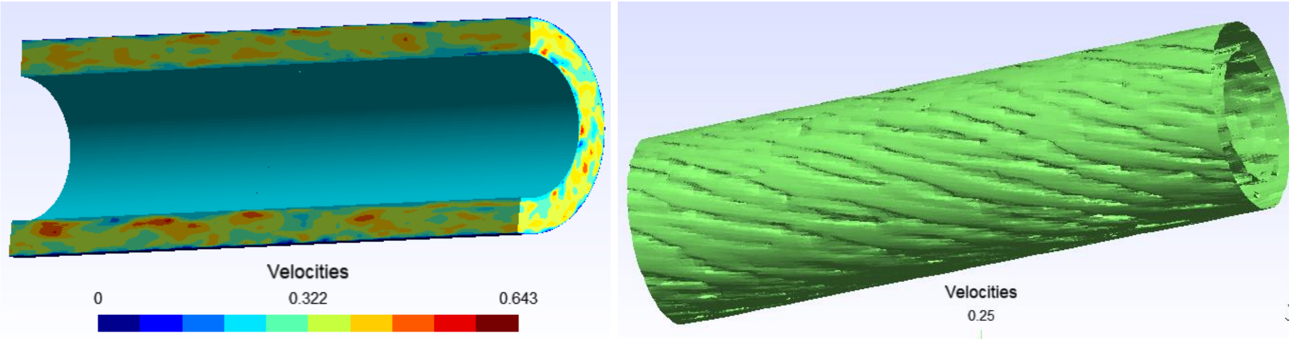

Figure 4.2: Velocity contours and velocity iso-surfaces for dp/dx= 62.2 Pa/m and rotation 44.6 rpm

The rotation causes an increase of the pressure drop, which can be seen in Figure 4.3 and Figure 4.4.

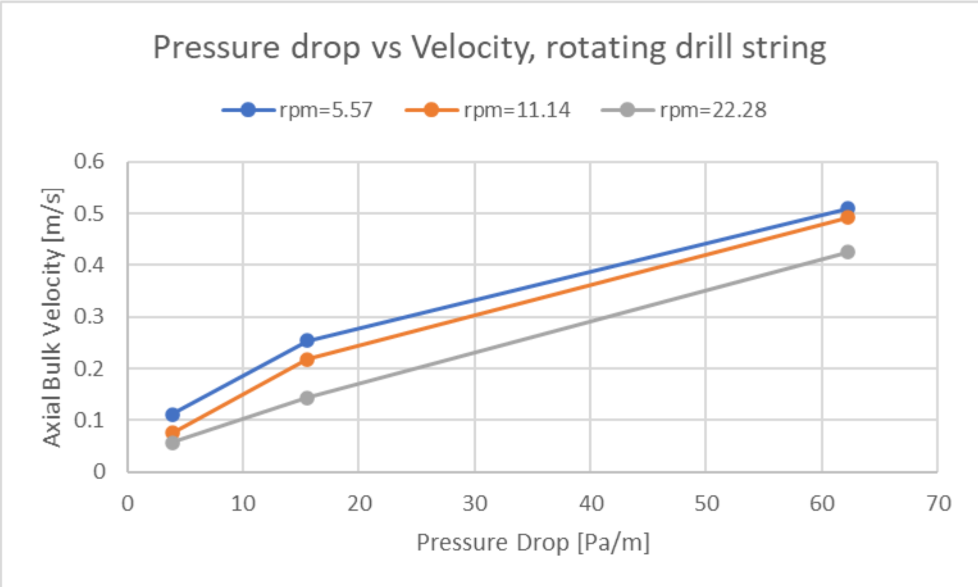

Figure 4.3: Axial bulk velocity vs. pressure drop

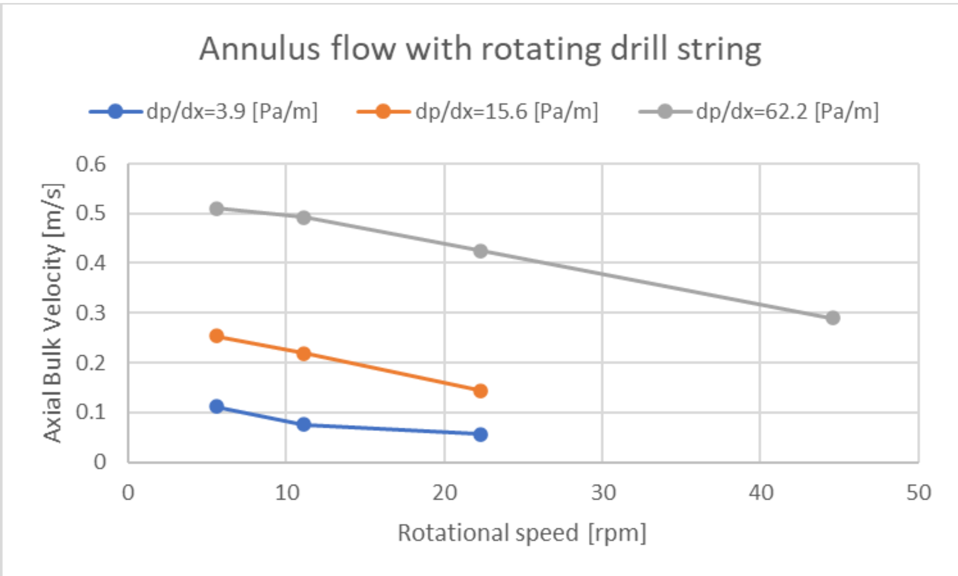

Figure 4.4: Axial bulk velocity vs. rotational speed

Similarly to Equation 3.2, it is possible to add the effect of rotation through a modified friction factor:

$$f_{annulus\_rotation} = k_{rotation} k_g f \quad (3.2)$$

This rotational friction correction factor has been plotted in Figure 4.5.

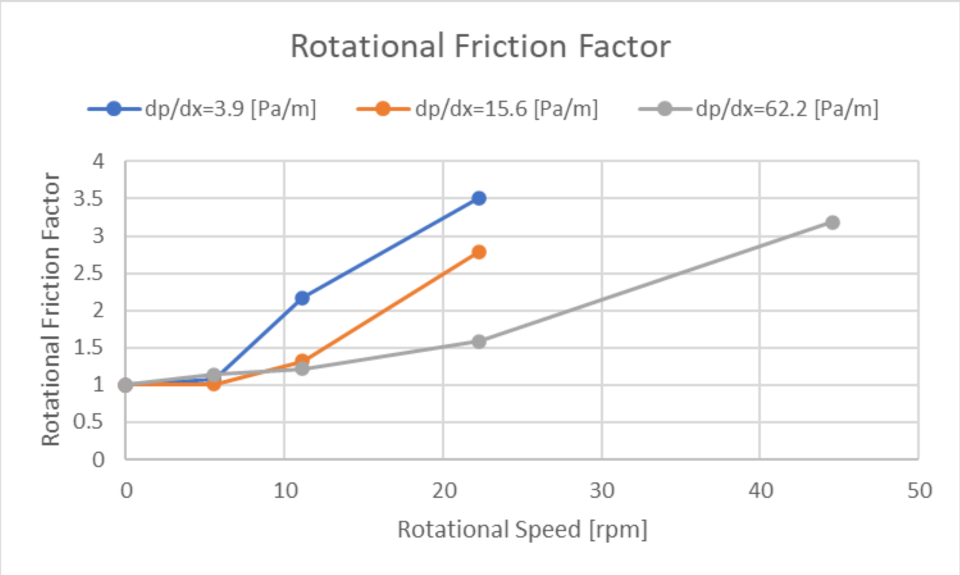

Figure 4.5: Rotational friction correction factor

5. CONCLUDING REMARKS

Laminar and turbulent flow simulations were carried out by 3D time-dependent LES for annular flow without and with rotation of the drill string. The overall approach was validated by comparison with 1D models for laminar and turbulent flows (without rotation). The approach forms a base for future development of models or correction terms such that pressure drops due to rotation, tool joints, sensor jackets, etc. can be taken into account. This will be particularly important when including non-Newtonian fluids, as it would be difficult to find relevant correction terms in the literature. It is important to note that this report will be updated and extended once more Geo-Drill experimental data become available.

6. REFERENCES

1. P. Kjellgren, C.B. Jenssen, H. Yu, T. Peng, GeoDrill deliverable report D7.1 ”Geothermal Well Flow Assurance Simulator”, Jan. 2021
2. P. Kjellgren, T. Peng, GeoDrill deliverable report D7.2 ”Drill String Physics Simulator”, Sept. 2021
3. PHREEQC Ver. 3; “A computer Program for Speciation, Batch-Reaction, One-Dimensional Transport, and Inverse Geochemical Calculations”, https://wwwbrr.cr.usgs.gov/projects/GWC_coupled/phreeqc/
4. P. Kjellgren, C.B. Jenssen, T. Peng, GeoDrill deliverable report D4.1 ”Design and simulation of fluidic amplifier”, Nov. 2019
5. P. Kjellgren, “A semi-implicit fractional step finite element method for viscous incompressible flows”, Computational Mechanics 20, 541–550 (1997). https://doi.org/10.1007/s004660050274